CONSTRAINED CAV CONTROL FOR MIXED VEHICULAR PLATOONS VIA GAIN PARAMETERIZATIONS AND PADÉ APPROXIMATIONS

MirSaleh Bahavarnia†, Junyi Ji†¶ Ahmad F. Taha†, and Daniel B. Work†¶

***Abstract*— The key objective of the connected and automated vehicle (CAV) platoon control problem is to regulate CAVs' position while ensuring stability and accounting for vehicle dynamics. The unconstrained version of this problem has thoroughly been investigated in the literature. We elaborate on the constrained version of this problem to theoretically mitigate the two shortcomings of the unconstrained counterpart: *(i)* the synthesis of unrealistic high-gain control parameters due to the lack of a systematic way to incorporate the lower and upper bounds on the control parameters, and *(ii)* the performance sensitivity to the communication delay due to inaccurate Taylor series approximation. The former is mitigated via a systematic parameterization of the control gains based on the Hurwitz stability criterion. The latter is mitigated by taking advantage of the well-known Padé approximation. The usefulness of the proposed theoretical results is assessed by performing numerous numerical simulations. Furthermore, a thorough comparative analysis is empirically conducted between the constrained and unconstrained versions of the CAV platoon control problem with application to the mixed vehicular platoon. Modern transportation systems will benefit from the proposed CAV controls by effectively attenuating the *stop-and-go disturbance*—a single cycle of deceleration followed by acceleration—amplification throughout the mixed vehicular platoon as it will potentially reduce collisions.**

***Index Terms*— Car-following models, connected and automated vehicles, $\mathcal{H}_\infty$ control, local stability, string stability, time-delay systems.**

I. INTRODUCTION AND PAPER CONTRIBUTIONS

TRAFFIC oscillations, also known as *stop-and-go disturbances*, in congested modes have recently attained growing attention (see [1] and the references therein). Stop-and-go disturbance refers to a single cycle of deceleration followed by acceleration. Several approaches have mainly been proposed to control human-driven vehicles. One promising approach is via variable speed limit (VSL) control [2], [3]. Another one utilizes the emerging connected and automated vehicle (CAV) technology facilitating the effective control of CAVs leading to prominent improvements in traffic flow capacity and stability [1], [4]–[6]. Specifically, the key objective of the *CAV platoon control problem* is to regulate CAVs' position while ensuring stability and accounting for vehicle longitudinal dynamics [1].

The CAV technology [7], essential for improving road safety and efficiency, deeply hinges on the efficacy of vehicle-to-everything (V2X) communication systems. Both dedicated short-range communications and cellular vehicle-to-everything technologies can efficiently support safety applications necessitating end-to-end latency of around 100 milliseconds, provided that vehicle density remains within reasonable limits [8]. However, a vital challenge arises as traffic density escalates, leading to a marked increase in V2X communication delay due to the communication channel congestion, as highlighted in various studies [9]–[11]. This surge in latency, specifically in congested scenarios, is crucial. As detailed by [11], effective vehicle platooning must accommodate maximum latencies ranging from 10 to 500 milliseconds. This necessitates the development of advanced control systems capable of adapting to these varying delay conditions, thereby ensuring the reliability and safety of vehicle platooning in different traffic environments.

Although the CAV platoon control problem has thoroughly been studied in the literature, the existing research work [1] has some shortcomings. Two main shortcomings include *(i)* the synthesis of unrealistic high-gain control parameters due to the lack of a systematic way to incorporate the lower and upper bounds on the control parameters (also known as box constraints), and *(ii)* the performance sensitivity to the communication delay due to inaccurate Taylor series approximation.

Main Contributions. The main contributions of this paper can be listed as follows: *1)* To effectively address such shortcomings, taking advantage of the well-known Padé approximation, this paper presents a constrained CAV platoon controller synthesis that *(i)* systematically incorporates the lower and upper bounds on the control parameters, and *(ii)* significantly improves the performance sensitivity to the communication delay, *2)* Given the box constraints, we parameterize the locally stabilizing gains and then ensuring the additional string stability criterion, we obtain more representative parameterized locally stabilizing gains. The Padé approximation facilitates ensuring the string stability criterion in the presence of communication delay which leads to a better sub-optimality compared to the Taylor series approximation, and *3)* Minimizing the $\mathcal{H}_\infty$ norm of the Padé approximated transfer function over an interval defined by predominant acceleration frequency boundaries of human-driven vehicles, we solve for a sub-optimal constrained CAV platoon controller synthesis via nonlinear optimization tools. A thorough comparative analysis is empirically conducted between the constrained and unconstrained versions of the CAV platoon control problem with application to the mixed vehicular platoon.

The rest of the paper is organized as follows: Section II formally presents the preliminaries and the problem statement. Section III includes the main results followed by the numerous numerical simulations detailed by Section IV. At last, Section V concludes the paper with a few concluding remarks.

Paper Notations. The uppercase and lowercase letters denote the matrices and vectors, respectively. We represent the supremum and maximum by $\sup$ and $\max$, respectively. The set of n-dimensional real-valued vectors is symbolized by $\mathbb{R}^n$. For a vector $v \in \mathbb{R}^n$, we denote its ℓ_∞ norm (i.e., $\max_i |v_i|$) by $\|v\|_{\ell_\infty}$. We represent the vector of all ones with $\mathbf{1}$. To symbolize the imaginary unit, we use $j = \sqrt{-1}$. Also, to show the absolute value of a complex-valued number, we use $|.|$. For a square matrix M, we denote the set of its eigenvalues with $\lambda(M)$ and show its spectral abscissa (i.e., the

†The authors are with the Department of Civil and Environmental Engineering, Vanderbilt University, 2201 West End Avenue, Nashville, TN 37235, USA. ¶Institute for Software Integrated Systems. Emails: {mirsaleh.bahavarnia,junyi.ji,ahmad.taha,dan.work}@vanderbilt.edu.

This work is supported by the National Science Foundation, United States under grants ECCS 2151571, CMMI 2152450 and 2152928, and CNS 2135579.

maximum real part of its eigenvalues) by $\mathbf{sa}(M)$. A square matrix M is said to be Hurwitz if $\mathbf{sa}(M)<0$ holds. The time derivative of a signal $\chi(t)$ is represented by $\dot{\chi}(t)$.

II. Preliminaries and Problem Statement

Based on the preliminaries, we state a control problem to propose a constrained CAV platoon controller synthesis subject to the lower and upper bounds on the control parameters to avoid the synthesis of unrealistic high-gain control parameters. We also observe that communication delay can effectively be handled by utilizing a more accurate approximation (i.e., Padé approximation) for the delay-dependent exponential term. According to the travel direction, we consider a vehicular platoon consisting of N_{vp} vehicles with vehicle 1 and vehicle N_{vp} as the most preceding and the most following vehicles, respectively.

A. Preliminaries

1) State-space representation: Consider the state-space representation of the CAV system i as follows [1], [12], [13]:

$$\dot{\chi}_i(t)=A_i\chi_i(t)+B_iu_i(t)+Da_{i-1}(t), \tag{1}$$
$$A_i=\begin{bmatrix}0 & 1 & -\tau_i^*\\ 0 & 0 & -1\\ 0 & 0 & -\frac{1}{T_i}\end{bmatrix}, B_i=\begin{bmatrix}0\\ 0\\ \frac{K_i}{T_i}\end{bmatrix}, D=\begin{bmatrix}0\\ 1\\ 0\end{bmatrix},$$

where $\chi_i(t)=\begin{bmatrix}\sigma_i(t) & \Delta v_i(t) & a_i(t)\end{bmatrix}^\top$, $\sigma_i(t):=\Delta\vartheta_i(t)-\Delta\vartheta_i^*(t)$, $\Delta v_i(t):=v_{i-1}(t)-v_i(t)$, $a_i(t)$, and $u_i(t)$ denote the state vector, the deviation from equilibrium spacing, the speed difference with the preceding vehicle (i.e., vehicle $i-1$), the realized acceleration, and the control input, respectively (spacing is defined as $\Delta\vartheta_i(t):=\vartheta_{i-1}(t)-\vartheta_i(t)$). Furthermore, τ_i^*, T_i, and K_i represent the predefined constant time gap, time-lag for vehicle i to realize the acceleration, and ratio of demanded acceleration that can be realized, respectively. We can find an equilibrium state $\chi_{i,e}(t)$ by setting $\chi_i(t)=\chi_{i,e}(t)=\begin{bmatrix}0 & 0 & 0\end{bmatrix}^\top$. It is noteworthy that $a_{i-1}(t)$ is treated as an external disturbance for CAV system i.

To bypass multiple delay accumulation, we utilize the following standard decentralized linear control strategy [1]:

$$u_i(t)=\begin{bmatrix}k_{si} & k_{vi} & k_{ai}\end{bmatrix}\chi_i(t)+k_{fi}a_{i-1}(t-\theta), \tag{2}$$

where k_{si}, k_{vi}, and k_{ai} respectively represent the feedback gains associated with the derivation from equilibrium spacing σ_i, the speed difference Δv_i, and the acceleration a_i. Moreover, k_{fi} and θ denote the feedforward gain and V2V/V2I communication delay, respectively. For brevity, we alternatively utilize $k=\begin{bmatrix}k_1 & k_2 & k_3 & k_4\end{bmatrix}$ to denote $k=\begin{bmatrix}k_{si} & k_{vi} & k_{ai} & k_{fi}\end{bmatrix}$. In a similar fashion, we simply represent A_i, B_i, K_i, T_i, and τ_i^* by A, B, K, T, and τ, respectively. The key objective of the linear control strategy (2) is to regulate CAVs' position while ensuring stability and accounting for vehicle longitudinal dynamics [1].

2) Local stability: Local stability (also known as internal stability) means that a disturbance (deviation from an equilibrium point) can locally be resolved by a system. In the context of a CAV system, it means that deviation from an equilibrium spacing, speed difference, and acceleration can locally be resolved in a vehicle [1].

Definition 1 (Local stability [1], [14]): A CAV platoon following a linear control strategy (e.g., the control strategy in (2)) is called locally stable for an equilibrium point χ_e if and only if $\mathbf{sa}(A+Bk)<0$ holds ($A+Bk$ is Hurwitz).

As Proposition 1 in [1] states, the CAV system in (1) governed by the control strategy in (2) is locally stable if the following inequalities are satisfied:

$$k_1>0,\ \tau k_1>-k_2,\ \frac{1}{K}>k_3,\ \left(\frac{1}{K}-k_3\right)(\tau k_1+k_2)>\frac{T}{K}k_1. \tag{3}$$

3) String stability: Strict string stability (also known as $\mathcal{H}_2$ norm string stability) means that the magnitude of a disturbance is not amplified for each leader-follower pair throughout a vehicular string [1].

Definition 2 (Strict string stability [1], [15]): A CAV platoon string is strict string stable if and only if

$$\|a_i(s)\|_2/\|a_{i-1}(s)\|_2\le 1,\ \forall i\in\mathcal{I}_{\text{CAV}},$$

hold where $\mathcal{I}_{\text{CAV}}$ denotes the set of CAVs and $\|a_i(s)\|_2$ represents the $\mathcal{H}_2$ norm of $a_i(s)$ which is defined as $\|a_i(s)\|_2:=\sqrt{\int_0^\infty|a_i(j\omega)|^2d\omega}$.

Applying the following Cauchy inequality [1], [15]:

$$\|a_i(s)\|_2/\|a_{i-1}(s)\|_2\le\|a_i(s)/a_{i-1}(s)\|_\infty,$$

a sufficient condition to guarantee the string stability can be derived as

$$\|F_i(s)\|_\infty:=\sup_{\omega>0}|F_i(j\omega)|\le 1, \tag{4}$$

where $F_i(s):=\frac{a_i(s)}{a_{i-1}(s)}$ and $\|F_i(s)\|_\infty$ represent the transfer function capturing disturbance propagation throughout the vehicular string in the frequency domain and its $\mathcal{H}_\infty$ norm (i.e., the upper bound of the disturbance propagation ratio throughout the vehicular string), respectively. By taking the Laplace transform of the closed-loop system consisting of (1) and (2), one can obtain the following expression for $F_i(s)$:

$$F_i(s)=\frac{K(k_4s^2e^{-\theta s}+k_2s+k_1)}{c_3s^3+c_2s^2+c_1s+c_0}, \tag{5}$$
$$c_3=T,\ c_2=-Kk_3+1,\ c_1=K(\tau k_1+k_2),\ c_0=Kk_1.$$

Substituting $s=j\omega$ in (5), one can analytically compute $|F_i(j\omega)|$ as detailed by [16]. The exponential term associated with the communication delay θ in $F_i(s)$ in (5), i.e., $e^{-\theta s}$, adds more complexity to the $\mathcal{H}_\infty$ controller synthesis, necessitating the utilization of approximation techniques to efficiently compute the approximate value of $\|F_i(s)\|_\infty$. In that regard, diverse approximations exist. For instance, the authors in [1], based on a sufficient condition (i.e., utilizing the Taylor series approximations of $\cos(\theta\omega)\approx 1-\frac{\theta^2\omega^2}{2}$ and $\sin(\theta\omega)\approx\theta\omega-\frac{\theta^3\omega^3}{6}$ for a sufficiently small θ) and imposing the sufficient condition (4), derive a set of inequalities presented by Proposition 2 in [1] as

$$T^2+\frac{K^2k_4k_2\theta^3}{3}\ge 0, \tag{6a}$$
$$-2KT(\tau k_1+k_2)+(Kk_3-1)^2-K^2k_4(k_1\theta^2+2k_2\theta+k_4)\ge 0, \tag{6b}$$
$$2Kk_1\left(K\left(k_4+k_3+\tau k_2+\frac{\tau^2k_1}{2}\right)-1\right)\ge 0, \tag{6c}$$

to guarantee the string stability of the CAV system in (1) governed by the control strategy in (2) for a sufficiently small θ.

B. Problem statement

The ultimate goal of the current study is to apply the CAV platoon controller synthesis results to the mixed vehicular platoon. Due to the string unstable behavior of human-driven vehicles, we have no direct control over them. Nonetheless, applying the (fully) CAV platoon controller synthesis results to the mixed vehicular platoon can effectively attenuate the stop-and-go disturbance amplification throughout the mixed vehicular platoon. In the case of the mixed vehicular platoon, the frequency of human-driven vehicle acceleration throughout traffic oscillations is bounded and typically shows a predominant range [1], [17]. Then, for practicality, we aim at minimizing $\|F_i(s)\|_\infty$ over an interval defined by predominant

acceleration frequency boundaries of human-driven vehicles (see [1] for more details). Given the transfer function $F_i(s)=\frac{a_i(s)}{a_{i-1}(s)}$ and the predominant acceleration frequency boundaries of human-driven vehicles, namely $\omega_2>\omega_1>0$, let us define/denote its $\mathcal{H}_\infty$ norm over $\omega\in[\omega_1,\omega_2]$, namely $\mathcal{H}_\infty^{[\omega_1,\omega_2]}$, as [1]

$$\|F_i(s)\|_\infty^{[\omega_1,\omega_2]}:=\sup_{\omega\in[\omega_1,\omega_2]}|F_i(j\omega)|. \tag{7}$$

Observe that based on definitions (4) and (7), inequalities $\|F_i(s)\|_\infty^{[\omega_1,\omega_2]}\leq\|F_i(s)\|_\infty\leq 1$ are satisfied if (4) holds. Defining the $\mathcal{H}_\infty$ norm over the predominant acceleration frequency boundaries of human-driven vehicles $\omega_2>\omega_1>0$, we are now ready to formally state the main problem to be investigated in this paper.

Problem 1: Given the CAV system in (1) governed by the control strategy in (2), the predominant acceleration frequency boundaries of human-driven vehicles $\omega_2>\omega_1>0$, and the following *box constraints* (i.e., the lower and upper bounds) on the gains $\begin{bmatrix}k_1 & k_2 & k_3 & k_4\end{bmatrix}$:

$$k_i^l\leq k_i\leq k_i^u,\ i\in\{1,2,3\}, \tag{8a}$$

$$k_4^l\leq k_4\leq k_4^u, \tag{8b}$$

synthesize an $\mathcal{H}_\infty^{[\omega_1,\omega_2]}$ optimal control strategy with an optimal $\mathcal{H}_\infty^{[\omega_1,\omega_2]}$ norm of γ ($\gamma\leq 1$).

Solving Problem 1 facilitates the effective attenuation of the stop-and-go disturbance amplification throughout the mixed vehicular platoon over the predominant acceleration frequency boundaries of human-driven vehicles. Furthermore, such a controller synthesis *(i)* facilitates the effective stop-and-go disturbance attenuation for the scenario with a large communication delay, and *(ii)* systematically incorporates the box constraints arising from the physics of the problem. Remarkably, these objectives are not achievable via the controller synthesis proposed by [1].

III. Main Results

By parameterizing locally stabilizing gains subject to box constraints, first, we systematically incorporate the local stability and the box constraints. Second, we additionally ensure the string stability via the Padé approximation. Finally, built upon the previous two steps, we efficiently solve for a sub-optimal solution to Problem 1. For the proofs, see Appendices A–C in [16].

A. Parameterized locally stabilizing gains

The set of feedback gains $\begin{bmatrix}k_1 & k_2 & k_3\end{bmatrix}$ satisfying the local stability (3) can be parameterized via the parameters $\begin{bmatrix}x & y & z\end{bmatrix}$ as

$$k_1(x)=x,\ k_2(x,y)=-\tau x+y,\ k_3(x,y,z)=\frac{-Tx+y}{Ky}-z, \tag{9}$$

where x, y, and z are all positive parameters. Imposing box constraints (8a) to the parameterization (9), we obtain the parameterization of the parameters x, y, and z in (9) detailed by Proposition 1 in [16]. Similar to Proposition 1 in [16], the feedforward gain k_4 satisfying box constraint (8b) can simply be parameterized via the parameter ψ_4 as $k_4=(1-\psi_4)k_4^l+\psi_4 k_4^u$, where $\psi_4\in[0,1]$ holds. Note that the form of ψ_i's for all $i\in\{1,2,3,4\}$ can be chosen via any arbitrary sigmoid function, e.g., the logistic function $\psi(\beta)=\frac{1}{1+e^{-\zeta\beta}}$, where $\zeta>0$ denotes the logistic growth rate. According to the statement of Lemma 1 in [16], if the sufficient condition on the string stability (4) holds for the transfer function $F_i(s)$ in (5), then inequality (6c) holds for the control parameters $\begin{bmatrix}k_1 & k_2 & k_3 & k_4\end{bmatrix}$. Utilizing the necessary condition (associated with the string stability) stated by Lemma 1 in [16], i.e., inequality (6c), and noting that $K>0$ and $k_1>0$ hold, the feedforward gain k_4 can be parameterized via the parameters $\begin{bmatrix}x & y & z & w\end{bmatrix}$ as $k_4(x,y,z,w)=\frac{\tau^2 x}{2}-\tau y+\frac{Tx}{Ky}+z+w$, where x, y, and z are as expressed in (9) and w is a non-negative parameter. Imposing box constraints (8) to the parameterizations (9) and $k_4(x,y,z,w)=\frac{\tau^2 x}{2}-\tau y+\frac{Tx}{Ky}+z+w$, we obtain the following parameterization of the parameters x, y, z, and w in (9) and $k_4(x,y,z,w)=\frac{\tau^2 x}{2}-\tau y+\frac{Tx}{Ky}+z+w$:

TABLE I

Closed-form expressions for the parameters in Propositoin 1.

$x^l=\max\{\epsilon,k_1^l\},\ x^u=k_1^u$
$y_{\psi_1}^l=\max\left\{\epsilon,\tau\mathtt{x}(\psi_1)+k_2^l,\frac{T\mathtt{x}(\psi_1)}{-Kk_3^l+1-K\epsilon},\phi_y\right\},\ y_{\psi_1}^u=\tau\mathtt{x}(\psi_1)+k_2^u$
$z_{\psi_1,\psi_2}^l=\max\left\{\epsilon,\frac{-T\mathtt{x}(\psi_1)+\mathtt{y}(\psi_1,\psi_2)}{K\mathtt{y}(\psi_1,\psi_2)}-k_3^u\right\}$
$z_{\psi_1,\psi_2}^u=\min\left\{\frac{-T\mathtt{x}(\psi_1)+\mathtt{y}(\psi_1,\psi_2)}{K\mathtt{y}(\psi_1,\psi_2)}-k_3^l,\phi_z\right\}$
$w_{\psi_1,\psi_2,\psi_3}^l=\max\{0,\phi_w\}$
$w_{\psi_1,\psi_2,\psi_3}^u=\frac{-\tau^2\mathtt{x}(\psi_1)}{2}+\tau\mathtt{y}(\psi_1,\psi_2)+\frac{-T\mathtt{x}(\psi_1)}{K\mathtt{y}(\psi_1,\psi_2)}-\mathtt{z}(\psi_1,\psi_2,\psi_3)+k_4^u$
ϵ: an infinitesimal positive value
$\phi_y=\frac{\xi(\mathtt{x}(\psi_1))+\sqrt{\xi(\mathtt{x}(\psi_1))^2+\frac{4T\tau\mathtt{x}(\psi_1)}{K}}}{2\tau},\ \xi(\mathtt{x}(\psi_1))=\frac{\tau^2\mathtt{x}(\psi_1)}{2}+\epsilon-k_4^u$
$\phi_z=\frac{-\tau^2\mathtt{x}(\psi_1)}{2}+\tau\mathtt{y}(\psi_1,\psi_2)+\frac{-T\mathtt{x}(\psi_1)}{K\mathtt{y}(\psi_1,\psi_2)}+k_4^u$
$\phi_w=\frac{-\tau^2\mathtt{x}(\psi_1)}{2}+\tau\mathtt{y}(\psi_1,\psi_2)+\frac{-T\mathtt{x}(\psi_1)}{K\mathtt{y}(\psi_1,\psi_2)}-\mathtt{z}(\psi_1,\psi_2,\psi_3)+k_4^l$

Proposition 1: The parameters $\begin{bmatrix}x & y & z & w\end{bmatrix}$ in (9) and $k_4(x,y,z,w)=\frac{\tau^2 x}{2}-\tau y+\frac{Tx}{Ky}+z+w$ satisfying box constraints (8) can be parameterized via the parameters $\begin{bmatrix}\psi_1 & \psi_2 & \psi_3 & \psi_4\end{bmatrix}$ as

$$\begin{aligned}
&x=\mathtt{x}(\psi_1)=(1-\psi_1)x^l+\psi_1 x^u,\\
&y=\mathtt{y}(\psi_1,\psi_2)=(1-\psi_2)y_{\psi_1}^l+\psi_2 y_{\psi_1}^u,\\
&z=\mathtt{z}(\psi_1,\psi_2,\psi_3)=(1-\psi_3)z_{\psi_1,\psi_2}^l+\psi_3 z_{\psi_1,\psi_2}^u,\\
&w=\mathtt{w}(\psi_1,\psi_2,\psi_3,\psi_4)=(1-\psi_4)w_{\psi_1,\psi_2,\psi_3}^l+\psi_4 w_{\psi_1,\psi_2,\psi_3}^u,
\end{aligned} \tag{10}$$

where $\psi_i\in[0,1]$ holds for all $i\in\{1,2,3,4\}$ and the expressions for x^l, x^u, $y_{\psi_1}^l$, $y_{\psi_1}^u$, z_{ψ_1,ψ_2}^l, z_{ψ_1,ψ_2}^u, $w_{\psi_1,\psi_2,\psi_3}^l$, and $w_{\psi_1,\psi_2,\psi_3}^u$ are reflected on Tab. I.

Merging (9), $k_4(x,y,z,w)=\frac{\tau^2 x}{2}-\tau y+\frac{Tx}{Ky}+z+w$, and (10) along with sigmoid functions, we obtain the following parameterization of the locally stabilizing gains $\begin{bmatrix}k_1 & k_2 & k_3 & k_4\end{bmatrix}$ subject to box constraints (8):

Corollary 1: The locally stabilizing gains $\begin{bmatrix}k_1 & k_2 & k_3 & k_4\end{bmatrix}$ subject to box constraints (8) can be parameterized via the parameters $\begin{bmatrix}\kappa_1 & \kappa_2 & \kappa_3 & \kappa_4\end{bmatrix}$ as

$$\begin{aligned}
&k_1(\kappa_1)=\mathtt{x}(\psi(\kappa_1)),\\
&k_2(\kappa_1,\kappa_2)=-\tau\mathtt{x}(\psi(\kappa_1))+\mathtt{y}(\psi(\kappa_1),\psi(\kappa_2)),\\
&k_3(\kappa_1,\kappa_2,\kappa_3)=\frac{-T\mathtt{x}(\psi(\kappa_1))+\mathtt{y}(\psi(\kappa_1),\psi(\kappa_2))}{K\mathtt{y}(\psi(\kappa_1),\psi(\kappa_2))}\\
&\quad-\mathtt{z}(\psi(\kappa_1),\psi(\kappa_2),\psi(\kappa_3)),\\
&k_4(\kappa_1,\kappa_2,\kappa_3,\kappa_4)=\frac{\tau^2\mathtt{x}(\psi(\kappa_1))}{2}-\tau\mathtt{y}(\psi(\kappa_1),\psi(\kappa_2))\\
&\quad+\frac{T\mathtt{x}(\psi(\kappa_1))}{K\mathtt{y}(\psi(\kappa_1),\psi(\kappa_2))}+\mathtt{z}(\psi(\kappa_1),\psi(\kappa_2),\psi(\kappa_3))\\
&\quad+\mathtt{w}(\psi(\kappa_1),\psi(\kappa_2),\psi(\kappa_3),\psi(\kappa_4)),
\end{aligned} \tag{11}$$

where $\kappa_i\in\mathbb{R}$ holds for all $i\in\{1,2,3,4\}$ and $\mathtt{x}()$, $\mathtt{y}()$, $\mathtt{z}()$, and $\mathtt{w}()$ represent the same functions expressed in (10).

Given the locally stabilizing gains $\begin{bmatrix}k_1 & k_2 & k_3 & k_4\end{bmatrix}$ subject to box constraints (8) and utilizing the parameterization (11), the corresponding parameters $\begin{bmatrix}\kappa_1 & \kappa_2 & \kappa_3 & \kappa_4\end{bmatrix}$ can be extracted as

detailed by Corollary 3 in [16]. As a summary, *(i)* Corollary 1 will be utilized as a cornerstone to parameterize the locally stabilizing gains $\begin{bmatrix} k_1 & k_2 & k_3 & k_4 \end{bmatrix}$ via the parameters $\begin{bmatrix} \kappa_1 & \kappa_2 & \kappa_3 & \kappa_4 \end{bmatrix}$, and *(ii)* Corollary 3 in [16] will facilitate the extraction of the parameters $\begin{bmatrix} \kappa_1 & \kappa_2 & \kappa_3 & \kappa_4 \end{bmatrix}$ given the locally stabilizing gains $\begin{bmatrix} k_1 & k_2 & k_3 & k_4 \end{bmatrix}$. The former is useful for searching for the sub-optimal solution to Problem 1 while the latter is essential for opting (extracting) an initial feasible point for the main optimization problem associated with Problem 1.

B. String stability via the Padé approximation

As mentioned earlier, one needs to overcome the complexity of the communication delay in the $\mathcal{H}_\infty$ controller synthesis. To that end, unlike the Taylor series approximation utilized by [1], we employ the Padé approximation approach to approximate the transfer function $F_i(s)$ in (5), namely $\hat{F}_i(s)$. For more details, see Section III-B in [16].

Inspired by the sufficient condition (4), to more accurately ensure the string stability of the CAV system in (1) governed by the control strategy in (2) in the presence of communication delay, we utilize the following condition: $\|\hat{F}_i(s)\|_\infty \leq 1$. Centering around $\|\hat{F}_i(s)\|_\infty \leq 1$, we incorporate the string stability into the locally stabilizing box-constrained gains by utilizing the Padé approximation. Although an analytical explicit formula exists for $F_i(j\omega)$ in (4) and (7), utilizing the approximate forms of (4) and (7) via the Padé approximation, is unavoidable as (4) and (7) cannot directly be utilized due to the computational complexity of computing $\|F_i(s)\|_\infty$ and $\|F_i(s)\|_\infty^{[\omega_1,\omega_2]}$, respectively. Then, in the next section, we alternatively utilize the Padé approximation-based counterparts $\|\hat{F}_i(s)\|_\infty$ and $\|\hat{F}_i(s)\|_\infty^{[\omega_1,\omega_2]}$ to effectively solve Problem 1 for a sub-optimal solution.

C. A sub-optimal solution to Problem 1

We here propose a two-stage procedure to solve Problem 1 for a sub-optimal solution. Substituting the parameterized locally stabilizing gains (11) provided by Corollary 1 into $F_i(s)$ in (5), we obtain the parameterized $F(s;\kappa)$ and denote its Padé approximation by $\hat{F}(s;\kappa)$. Then, defining the optimization variable κ as $\kappa := \begin{bmatrix} \kappa_1 & \kappa_2 & \kappa_3 & \kappa_4 \end{bmatrix}^\top$, we first consider the following optimization problem:

$$\underset{\kappa\in\mathbb{R}^4}{\text{Minimize}}\ \|\hat{F}(s;\kappa)\|_\infty^{[\omega_1,\omega_2]}, \tag{12a}$$

$$\text{subject to:}\ \|\hat{F}(s;\kappa)\|_\infty \leq 1, \tag{12b}$$

to solve Problem 1 for a sub-optimal solution. We then propose a two-stage procedure as follows:

1) We first search for an initial stabilizing feasible point κ^0 that satisfies constraint (12b).
2) We then solve optimization problem (12) for a sub-optimal solution κ^* starting from the obtained initial stabilizing feasible point in the first stage, i.e., κ^0. Finally, one can compute k^* by substituting κ^* into the parameterization (11) provided by Corollary 1 as $k^* = k(\kappa^*)$.

In the sequel, we delve into each stage thoroughly.

1) First stage: Notably, one can take advantage of Corollary 3 in [16] to extract κ^0 from k^0. Such a fact motivates us to: first, alternatively search for an initial stabilizing feasible point k^0 and second, extract the corresponding initial stabilizing feasible point κ^0 from k^0. To that end, first, we consider the following parameterization:

$$\begin{aligned} k_1(\mu_1) &= (1-\rho(\mu_1))\max\{\epsilon, k_1^l\} + \rho(\mu_1)k_1^u, \\ k_i(\mu_i) &= (1-\rho(\mu_i))k_i^l + \rho(\mu_i)k_i^u,\ i\in\{2,3,4\}, \end{aligned} \tag{13}$$

with $\rho(\beta) = \frac{1}{1+\nu\beta^2}$ where $\nu > 0$ can arbitrarily be chosen and second, defining $\mu := \begin{bmatrix} \mu_1 & \mu_2 & \mu_3 & \mu_4 \end{bmatrix}^\top$ and substituting the parameterized gains (13) into $F_i(s)$ in (5), we obtain the parameterized $G(s;\mu)$ and denote its Padé approximation by $\hat{G}(s;\mu)$. Then, to search for an initial stabilizing feasible point μ^0 that satisfies $\|\hat{G}(s;\mu)\|_\infty \leq 1$ (an equivalent constraint to constraint (12b)), we solve the following standard $\mathcal{H}_\infty$ optimization problem:

$$\underset{\mu\in\mathbb{R}^4}{\text{Minimize}}\ \|\hat{G}(s;\mu)\|_\infty, \tag{14}$$

for μ^0, utilizing a well-developed standard $\mathcal{H}_\infty$ problem solver, namely `hinfstruct` solver. Afterwards, according to the parameterization (13), we get $k^0 = k(\mu^0)$ and plug k^0 to Corollary 3 in [16] to extract κ^0.

2) Second stage: Motivated by $\|\hat{F}_i(s)\|_\infty \leq 1$, let us define the following function:

$$h(\kappa) := \begin{cases} \|\hat{F}(s;\kappa)\|_\infty^{[\omega_1,\omega_2]} & \text{if } \|\hat{F}(s;\kappa)\|_\infty \leq 1, \\ \alpha & \text{else}, \end{cases} \tag{15}$$

where $\alpha > 1$ can arbitrarily be chosen. Now, we alternatively solve the following unconstrained optimization problem:

$$\underset{\kappa\in\mathbb{R}^4}{\text{Minimize}}\ h(\kappa), \tag{16}$$

to find a solution κ^* to optimization problem (12). Finally, one can compute k^* by substituting κ^* into the parameterization (11) provided by Corollary 1 as $k^* = k(\kappa^*)$. Regarding the initialization, we utilize κ^0 obtained from the first stage. Furthermore, due to the non-convex and non-smooth nature of the function $h(\kappa)$ in (15), we need to utilize non-convex and non-smooth optimization tools to solve the unconstrained optimization problem (16). For instance, we can employ `fminsearch` solver. Procedure 1 summarizes the two-stage $\mathcal{H}_\infty$ controller synthesis procedure.

Procedure 1: *Two-stage $\mathcal{H}_\infty$ Controller Synthesis*

Input: $\tau, T, K, \theta, \omega_1, \omega_2, \{k_i^l\}_{i=1}^4, \{k_i^u\}_{i=1}^4, \alpha, \zeta, \nu, N$
First stage:
  Construct $G(s;\mu)$ via the parameterization (13).
  Get $\hat{G}(s;\mu)$ via the Padé approximation of $G(s;\mu)$.
  Solve (14) for μ^0 via `hinfstruct` solver.
  Compute $k^0 = k(\mu^0)$ via the parameterization (13).
  Extract κ^0 from k^0 via Corollary 3 in [16].
Second stage:
  Construct $F(s;\kappa)$ via the parameterization (11).
  Get $\hat{F}(s;\kappa)$ via the Padé approximation of $F(s;\kappa)$.
  Initialize (16) with κ^0 obtained from the first stage.
  Solve (16) for κ^* via `fminsearch` solver.
  Compute $k^* = k(\kappa^*)$ via the parameterization (11).
Output: k^*.

IV. Numerical Simulations

Throughout this section, we assess the effectiveness of the presented theoretical results via MATLAB simulations and the NGSIM trajectory data for I-80 in California [18]. Depending on how small the communication delay is, the section is divided into two main parts: *(a)* Case 1: a sufficiently small communication delay θ and *(b)* Case 2: a large communication delay θ. In Case 1,

TABLE II

THE TWO-STAGE $\mathcal{H}_\infty$ CONTROLLER SYNTHESIS k^* AND k^{unc} [1].

Vector	Value
k^*	$[0.4212 \quad 0.4775 \quad -1.0078 \quad 1.3197]^\top$
k^{unc}	$[0.9200 \quad 1.3200 \quad -0.9200 \quad 0.7200]^\top$

TABLE III

THE $\mathcal{H}_\infty^{[\omega_1,\omega_2]}$ NORM VALUES FOR k^{unc} [1] AND k^*.

ω_1	$\|F(s)\|_\infty^{[\omega_1,\omega_2]}$ for k^{unc}	$\|F(s)\|_\infty^{[\omega_1,\omega_2]}$ for k^*
0.1	0.9739	0.9628
0.3	0.9001	0.8207
0.5	0.8667	0.6758
0.7	0.7304	0.5669

since the communication delay θ is sufficiently small, we can set the unconstrained $\mathcal{H}_\infty$ controller synthesis proposed in [1], namely k^{unc}, as a benchmark for fair comparative analysis purposes. In that regard, to have a fair comparison, we impose the box constraints on k^*, based on $\|k^{\text{unc}}\|_{\ell_\infty}$. In other terms, we consider a hypercube that encompasses k^{unc}. In Case 2, since θ is not sufficiently small anymore, the Taylor series approximation-based method [1] becomes unusable. We utilize `getPeakGain` to evaluate the $\mathcal{H}_\infty^{[\omega_1,\omega_2]}/\mathcal{H}_\infty$ norm values. Regarding the Padé approximation, we utilize `pade` equipped with N which denotes the Padé approximation order. To utilize `hinfstruct`, we take advantage of `realp`, creating real-valued tunable parameters μ_1, μ_2, μ_3, and μ_4. Furthermore, we initialize those real-valued parameters via `rand`.

A. Case 1: a sufficiently small communication delay

In this section, for the sufficiently small θ, we conduct a comparative analysis between the unconstrained and constrained $\mathcal{H}_\infty$ syntheses k^{unc} [1] and k^*.

Similar to [1], we adopt the value setting from Tab. II in [16] for the experimental $\mathcal{H}_\infty$ controller synthesis. Time quantities are all in seconds. Setting $\omega_1 = 0.5$, $k^l = -\|k^{\text{unc}}\|_{\ell_\infty} [0 \quad 1 \quad 1 \quad 1]^\top$, $k^u = \|k^{\text{unc}}\|_{\ell_\infty} \mathbf{1}$, $\alpha = 1.05$, $\zeta = 5$, $\nu = 5$, $N = 5$ and running Procedure 1, we obtain the two-stage $\mathcal{H}_\infty$ controller synthesis k^* illustrated by Tab. II for which the $\mathcal{H}_\infty^{[\omega_1,\omega_2]}$ norm values corresponding to the unconstrained and constrained $\mathcal{H}_\infty$ syntheses k^* and k^{unc} [1] are $\|F(s)\|_\infty^{[\omega_1,\omega_2]} = 0.6758$ and $\|F(s)\|_\infty^{[\omega_1,\omega_2]} = 0.8667$, respectively.

According to $\lambda(A + Bk^*) = \{-8.0215, -0.4595 - 0.3606j, -0.4595 + 0.3606j\}$, and Fig. 1 in [16], we observe that box constraints (8) and both local stability (3) and string stability (4) are satisfied for k^*. As Fig. 2 in [16] depicts, the Padé approximation-based method attains a more accurate approximation than the Taylor series approximation-based counterpart.

For predominant acceleration frequency boundary of human-driven vehicles $\omega_1 \in \{0.1, 0.3, 0.5, 0.7\}$, Tab. III reflects the ω_1-dependency of the $\mathcal{H}_\infty^{[\omega_1,\omega_2]}$ norm values corresponding to the unconstrained and constrained $\mathcal{H}_\infty$ syntheses k^{unc} [1] and k^*.

Accordingly, for $\omega \in [0.01, 5.01]$, Fig. 1 illustrates the $|F(j\omega)|$ values corresponding to the unconstrained and constrained $\mathcal{H}_\infty$ syntheses k^{unc} [1] and k^* with $\theta = 0.1$ and $\omega_1 \in \{0.1, 0.3, 0.5, 0.7\}$.

According to Tab. III, the Padé approximation-based box-constrained solution outperforms the Taylor series approximation-based unconstrained solution [1] in terms of the $\mathcal{H}_\infty^{[\omega_1,\omega_2]}$ norm. As Fig. 1 depicts, although the unconstrained and constrained $\mathcal{H}_\infty$ syntheses have similar starting patterns, the patterns are different in the sequel. As an interesting observation, based on $\|F(s;\, \kappa^{\text{unc}}(0.5))\|_\infty^{[0.5,2.5]} = 0.8667$ and $\|F(s;\kappa^{\text{unc}}(0.3))\|_\infty^{[0.5,2.5]} = 0.8228$ from Fig. 1, we notice that inequality $\|F(s;\kappa^{\text{unc}}(0.5))\|_\infty^{[0.5,2.5]} \leq \|F(s;\kappa^{\text{unc}}(0.3))\|_\infty^{[0.5,2.5]}$ (due to definition (7)) is violated for the unconstrained $\mathcal{H}_\infty$ synthesis k^{unc} [1], i.e., for $\omega_1 = 0.5$, the sub-optimality of their proposed solution is high. It is noteworthy that such inequality violation does not occur in the case of constrained $\mathcal{H}_\infty$ synthesis k^* based on Fig. 1.

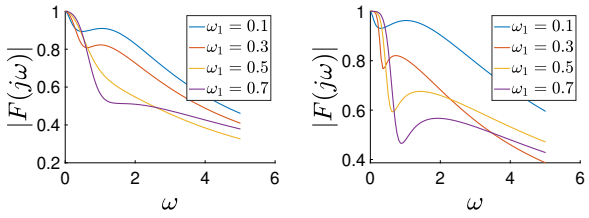

Fig. 1. The $|F(j\omega)|$ values for k^{unc} [1] on the left and k^* on the right with $\theta = 0.1$ and $\omega_1 \in \{0.1, 0.3, 0.5, 0.7\}$.

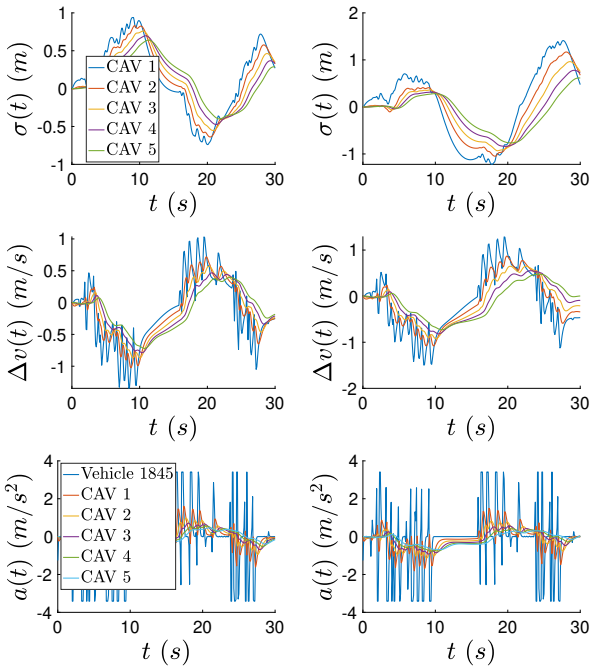

Fig. 2. The state trajectories corresponding to k^{unc} [1] on the left and k^* on the right with $\theta = 0.1$ and $\omega_1 = 0.3$.

To visualize the corresponding state trajectories of the unconstrained and constrained $\mathcal{H}_\infty$ syntheses k^{unc} [1] and k^*, we utilize the following formula:

$$\chi_i(t) = e^{(A_i+B_ik)t}\chi_i(0) + \int_0^t e^{(A_i+B_ik)(t-\varphi)}(B_ik_{fi}a_{i-1}(\varphi-\theta) + Da_{i-1}(\varphi))\, d\varphi,$$

along with the human-driven vehicle acceleration information adopted from the NGSIM trajectory data for I-80 in California [18]. Considering a mixed vehicular platoon consisting of 1 human-driven vehicle, namely Vehicle 1845 (as a leading vehicle) and 5 CAVs, and running Procedure 1 with $\theta = 0.1$ and $\omega_1 = 0.3$, we get the corresponding state trajectories of the unconstrained and constrained $\mathcal{H}_\infty$ syntheses k^{unc} [1] and k^* visualized in Fig. 2.

Moreover, Fig. 3 depicts the *Cumulative Damping Ratio* (defined as $\frac{\|a_i(s)\|_2}{\|a_0(s)\|_2}$ in [1]) associated with the CAVs for the unconstrained

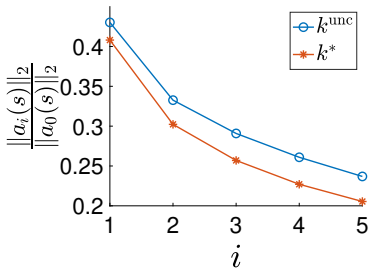

Fig. 3. The cumulative damping ratio associated with the CAVs for k^{unc} [1] and k^* with $\theta = 0.1$ and $\omega_1 = 0.3$.

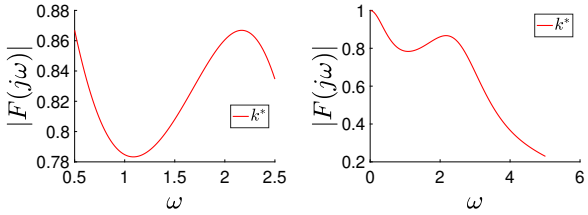

Fig. 4. The $|F(j\omega)|$ values for k^* with $\omega \in [\omega_1, \omega_2]$ on the left and $\omega \in [0.01, 5.01]$ on the right with $\theta = 1.5$ and $\omega_1 = 0.5$.

and constrained $\mathcal{H}_\infty$ syntheses k^{unc} [1] and k^* with $\theta = 0.1$ and $\omega_1 = 0.3$. Fig. 3 empirically certifies that the constrained $\mathcal{H}_\infty$ synthesis k^* outperforms the unconstrained $\mathcal{H}_\infty$ synthesis k^{unc} [1] in terms of disturbance attenuation effectiveness.

B. Case 2: a large communication delay

In this section, since θ is not sufficiently small anymore, the Taylor series approximation-based method [1] becomes unusable. We certify the functionality of the two-stage $\mathcal{H}_\infty$ controller synthesis procedure presented by Procedure 1 for dealing with large θ. Repeating the experiments for the value setting in Tab. II in [16] except for θ with $\theta = 1.5$, $\omega_1 = 0.5$, $k^l = -2\begin{bmatrix}0 & 1 & 1 & 1\end{bmatrix}^\top$, $k^u = \mathbf{21}$, $\alpha = 1.05$, $\zeta = 5$, $\nu = 5$, $N = 5$, we obtain the two-stage $\mathcal{H}_\infty$ controller synthesis k^* illustrated by Tab. V in [16] for which the $\mathcal{H}_\infty^{[\omega_1,\omega_2]}$ norm value corresponding to k^* is $\|F(s)\|_\infty^{[\omega_1,\omega_2]} = 0.8669$. Accordingly, for $\omega \in [\omega_1, \omega_2]$ on the left and $\omega \in [0.01, 5.01]$ on the right, Fig. 4 visualizes the $|F(j\omega)|$ values corresponding to the constrained $\mathcal{H}_\infty$ controller synthesis k^* with $\theta = 1.5$ and $\omega_1 = 0.5$. According to $\lambda(A + Bk^*) = \{-3.2621, -0.2376 - 0.3644j, -0.2376 + 0.3644j\}$, and Fig. 4, we realize that box constraints (8) and both local stability (3) and string stability (4) are satisfied for k^*.

V. Concluding Remarks

To effectively address the shortcomings arising from the unconstrained CAV platoon controller synthesis in the literature, this work proposes a (sub-optimal) constrained CAV platoon controller synthesis subject to the box constraints. Applying the (fully) CAV platoon controller synthesis results to the mixed vehicular platoon can effectively attenuate the stop-and-go disturbance amplification throughout the mixed vehicular platoon. Minimizing the $\mathcal{H}_\infty$ norm of the Padé approximated transfer function over an interval defined by predominant acceleration frequency boundaries of human-driven vehicles, we solve for a sub-optimal constrained CAV platoon controller synthesis via non-convex and non-smooth optimization tools. Conducting extensive numerical experiments certifies that *(i)* for a sufficiently small communication delay, the Padé approximation-based method outperforms the Taylor series approximation in terms of the $\mathcal{H}_\infty$ norm over an interval defined by predominant acceleration frequency boundaries of human-driven vehicles, and *(ii)* for a large communication delay, the Padé approximation-based method successfully proposes an $\mathcal{H}_\infty$ controller synthesis while the Taylor series approximation-based method in the literature becomes unusable.

Limitations: Although the sub-optimal performance of the proposed controller synthesis is satisfactory, its sub-optimality level can be sensitive to the first stage (stable initialization) of the proposed two-stage $\mathcal{H}_\infty$ controller synthesis procedure. As another limitation of the current study, we have assumed that the vehicle dynamics and the communication delay are deterministic and time-invariant, which is unrealistic. Elaboration on such a robust synthesis for the uncertain case can be considered as a pertinent future direction.

References

[1] Y. Zhou, S. Ahn, M. Wang, and S. Hoogendoorn, "Stabilizing mixed vehicular platoons with connected automated vehicles: An H-infinity approach," *Transportation Research Part B: Methodological*, vol. 132, pp. 152–170, 2020.

[2] A. Popov, A. Hegyi, R. Babuška, and H. Werner, "Distributed controller design approach to dynamic speed limit control against shockwaves on freeways," *Transportation Research Record*, vol. 2086, no. 1, pp. 93–99, 2008.

[3] A. Hegyi, S. P. Hoogendoorn, M. Schreuder, and H. Stoelhorst, "The expected effectivity of the dynamic speed limit algorithm specialist-a field data evaluation method," in *European Control Conference (ECC)*. IEEE, 2009, pp. 1770–1775.

[4] D. Chen, S. Ahn, M. Chitturi, and D. A. Noyce, "Towards vehicle automation: Roadway capacity formulation for traffic mixed with regular and automated vehicles," *Transportation Research Part B: Methodological*, vol. 100, pp. 196–221, 2017.

[5] G. Piacentini, A. Ferrara, I. Papamichail, and M. Papageorgiou, "Highway traffic control with moving bottlenecks of connected and automated vehicles for travel time reduction," in *IEEE 58th Conference on Decision and Control (CDC)*, 2019, pp. 3140–3145.

[6] S. C. Vishnoi, J. Ji, M. Bahavarnia, Y. Zhang, A. F. Taha, C. G. Claudel, and D. B. Work, "CAV traffic control to mitigate the impact of congestion from bottlenecks: A linear quadratic regulator approach and microsimulation study," *Journal on Autonomous Transportation Systems*, vol. 1, no. 2, pp. 1–37, 2024.

[7] E. Larsson, G. Sennton, and J. Larson, "The vehicle platooning problem: Computational complexity and heuristics," *Transportation Research Part C: Emerging Technologies*, vol. 60, pp. 258–277, 2015.

[8] R. Molina-Masegosa and J. Gozalvez, "LTE-V for sidelink 5G V2X vehicular communications: A new 5G technology for short-range vehicle-to-everything communications," *IEEE Vehicular Technology Magazine*, vol. 12, no. 4, pp. 30–39, 2017.

[9] K. C. Dey, A. Rayamajhi, M. Chowdhury, P. Bhavsar, and J. Martin, "Vehicle-to-vehicle (V2V) and vehicle-to-infrastructure (V2I) communication in a heterogeneous wireless network–performance evaluation," *Transportation Research Part C: Emerging Technologies*, vol. 68, pp. 168–184, 2016.

[10] S. A. Ahmad, A. Hajisami, H. Krishnan, F. Ahmed-Zaid, and E. Moradi-Pari, "V2V system congestion control validation and performance," *IEEE Transactions on Vehicular Technology*, vol. 68, no. 3, pp. 2102–2110, 2019.

[11] G. Naik, B. Choudhury, and J.-M. Park, "IEEE 802.11 bd & 5G NR V2X: Evolution of radio access technologies for V2X communications," *IEEE Access*, vol. 7, pp. 70 169–70 184, 2019.

[12] D. Swaroop, J. K. Hedrick, C. Chien, and P. Ioannou, "A comparison of spacing and headway control laws for automatically controlled vehicles," *Vehicle System Dynamics*, vol. 23, no. 1, pp. 597–625, 1994.

[13] K. Yi and Y. Do Kwon, "Vehicle-to-vehicle distance and speed control using an electronic-vacuum booster," *JSAE Review*, vol. 22, no. 4, pp. 403–412, 2001.

[14] R. E. Wilson and J. A. Ward, "Car-following models: Fifty years of linear stability analysis–a mathematical perspective," *Transportation Planning and Technology*, vol. 34, no. 1, pp. 3–18, 2011.

[15] G. J. Naus, R. P. Vugts, J. Ploeg, M. J. van De Molengraft, and M. Steinbuch, "String-stable cacc design and experimental validation: A frequency-domain approach," *IEEE Transactions on Vehicular Technology*, vol. 59, no. 9, pp. 4268–4279, 2010.

[16] M. Bahavarnia, J. Ji, A. F. Taha, and D. B. Work, "On the constrained CAV platoon control problem," *arXiv e-prints*, pp. arXiv–2401, 2024.

[17] C. Thiemann, M. Treiber, and A. Kesting, "Estimating acceleration and lane-changing dynamics from next generation simulation trajectory data," *Transportation Research Record*, vol. 2088, no. 1, pp. 90–101, 2008.

[18] *Next Generation Simulation (NGSIM) Vehicle Trajectories and Supporting Data. [Dataset]. Provided by ITS DataHub through Data.transportation.gov. Accessed 2024-03-11 from "http://doi.org/10.21949/1504477".*